Gene Expression, Vol. 16, pp. 39–47
Printed in the USA.

1052-2166/13 $90.00 + .00
DOI: http://dx.doi.org/10.3727/105221613X13806435102312
E-ISSN 1555-3884
www.cognizantcommunication.com

Determination of Relative Notch1 and γ-Secretase-Related Gene Expression in Puromycin-Treated Microdissected Rat Kidneys

Damir Simic, Frank Simutis, Catherine Euler, Christina Thurby, W. Mike Peden, R. Todd Bunch, Gary Pilcher, Thomas Sanderson, and Terry Van Vleet

Bristol-Myers Squibb Co., Drug Safety Evaluation, Mt. Vernon, IN, USA

Notch signaling pathways are involved in the regulation of cell differentiation and are highly conserved across species. Notch ligand binding leads to γ-secretase-mediated proteolytic cleavage of the Notch receptor releasing the Notch intracellular domain, resulting in its subsequent translocation into the nucleus and gene expression regulation. To investigate the level of expression of Notch signaling pathway components in microanatomic regions following renal injury, kidneys from untreated, vehicle control, and puromycin aminonucleoside (PA, 150 mg/kg)-treated rats were evaluated. Frozen tissue sections from rats were microdissected using laser capture microdissection (LCM) to obtain glomeruli, cortical (proximal) tubules, and collecting ducts, and relative gene expression levels of Presenilin1, Notch1, and Hes1 were determined. In untreated rats, the Notch1 expression in glomeruli was higher than in the proximal tubules and similar to that in collecting ducts, whereas Presenilin1 and Hes1 expressions were highest in the collecting ducts, followed by cortical tubules and glomeruli. Following PA-induced renal injury, Hes1 gene expression increased significantly in the glomeruli and tubules compared to the collecting ducts where no injury was observed microscopically. Although these data present some evidence of change in Notch signaling related to injury, the expression of Presenilin1, Notch1, and Hes1 in the microanatomic regions of the kidney following PA treatment were not significantly different when compared to controls. These results demonstrate that there are differences in Notch-related gene expression in the different microanatomic regions of the kidneys in rats and suggest a minimal role for Notch in renal injury induced by PA. In addition, this work shows that LCM coupled with the RT-PCR can be used to determine the relative differences in target gene expression within regions of a complex organ.

Key words: Laser capture microdissection LCM; RT-PCR; Puromycin; Kidney; Notch; γ-Secretase

INTRODUCTION

Gene expression analyses performed on whole organ homogenates from homogeneous tissues (such as liver) is a widely used technique; however, this method may result in "diluted" gene expression signatures, especially if expression of the genes of interest is limited to particular microanatomic regions. Laser capture microdissection coupled with RT-PCR can be used to determine relative differences in gene expression within microanatomic regions of heterogeneous organs such as the kidney. The basic functional unit of the kidney is the nephron, composed of a renal corpuscle that filters plasma into an elongated renal tubule. Within the renal corpuscle, a capillary tuft of fenestrated endothelial cells (the glomerulus) ensheathed by a layer of interdigitating podocytes filters plasma into Bowman's space. The filtrate composition is actively regulated as it flows from Bowman's space through proximal and distal tubules, collecting tubules, and collecting ducts.

γ-Secretase is a multisubunit protease complex consisting of four individual proteins: Presenilin1, Nicastrin, APH-1 (anterior pharynx defective-1 homolog), and PEN-2 (presenilin enhancer-2 homolog) (1). As an integral membrane protease, it has been implicated in the cleavage of numerous single-pass membrane proteins, most notably amyloid precursor protein (APP) and Notch. γ-Secretase-mediated cleavage of APP in the brain is associated with the amyloid fibrillogenesis and the accumulation of amyloid plaques implicated in the pathogenesis of Alzheimer's disease (2,3). γ-Secretase also cleaves the Notch transmembrane family of receptors that play a role in differentiation, development, maturation, and wound healing of numerous tissues and organ systems (4). Cleavage of Notch leads to the formation of its intracellular protein component, which translocates to the nucleus and regulates transcription via Hes, Hey, Deltex, and other transcription factors (5). There are few published studies regarding Notch-related pathways in the microanatomic

Address correspondence to Damir Simic, Bristol-Myers Squibb Co., Drug Safety Evaluation, 4601 Highway 62 East, Building 101 (P3), Mt. Vernon, IN 47620, USA. Tel: +1-812-307-2377; Fax: +1-812-307-2199; E-mail: damir.simic@bms.com *or* damir.simic@gmail.com

sections of the kidney, particularly during injury and repair. Most Notch signaling studies in the kidneys have been focused on the role of Notch in differentiation and development of the progenitor cells (6). It is commonly believed that, once kidney development is complete, there is little residual Notch activity in mature rodent and human kidneys (7,8). However, recent work has shown that Notch signaling in rodent and human adult kidneys can act as a regulator of differentiation and cellular commitment following an injury, chronic glomerular disorder, diabetes, or ongoing regeneration (9–12). Although likely important in regeneration/repair, some studies have shown that overexpression of the Notch intracellular domain and continual activation of Notch can lead to the rapid development of proteinuria, focal glomerulosclerosis, and death due to renal failure in rodent models (7,13).

In the glomerulus, it appears that the capacity for podocyte repair is limited and that, although acute Notch activation can aid in repair, sustained Notch expression and activation in podocytes is maladaptive, inducing glomerulosclerosis (14). Mature podocytes cannot proliferate, and if the injury is minimal, they generally increase in size to maintain the glomerular filtration barrier. However, if injury is severe (i.e., >20% of podocytes lost), podocytes can be replaced by renal progenitor cells (15,16). The differentiation of renal progenitor cells to podocytes involves the Notch signaling pathway (9,17). The location and presence of kidney progenitor cells has been debated (16,18,19); however, recently they have been described in the urinary pole of Bowman's capsule (16,20).

Puromycin aminonucleoside (PA) treatment in rats represents an experimental model of human minimal change disease (MCD) and focal segmental glomerulosclerosis (FSGS) (21,22). The extent of glomerular injury and onset of proteinuria depends on the strain of rat, route of administration, and dosing schedule. An intravenous single dose of 150 mg/kg PA induces reversible proteinuria peaking around day 10 with ultrastructural EM (transmission electron microscopy) changes of podocyte foot process effacement and detachment from the basement membrane that are consistent with MCD in humans (23). The proteinuria in this model is likely due to flattening and loss of foot processes, damage to the slit diaphragm, and eventual loss of size and charge selectivity in podocytes. Although 5 days of subcutaneous PA treatment at 15 mg/kg in rats leads to reversible MCD-like glomerular lesions, 10 days of treatment leads to the development of irreversible glomerulosclerosis (24). Overall, a higher cumulative PA dose leads to increased severity of the glomerular injury with the eventual induction of FSGS including podocyte detachment and apoptosis (25). The mechanism of PA-induced glomerular injury seems to originate from the generation of reactive oxygen species causing oxidative damage and DNA adducts (26–28). Elegant studies have shown that rats pretreated with oxygen radical scavengers were less susceptible to PA-induced glomerular injury and showed reduced proteinuria and podocyte injury (28,29). To evaluate the role of the Notch pathway in the microdissected regions of the kidney prior to and following a PA-induced injury, this study utilized LCM coupled with RT-PCR to assess Presenilin1, Notch1, and Hes1 relative gene expression. The present study utilized the Olson et al. (23) glomerular (podocyte) injury model by intravenously treating female rats with a single dose of PA (150 mg/kg). At day 10 postdose, microdissected sections (glomeruli, cortical tubules, and collecting ducts) were evaluated for the expression of Presenilin1 (γ-secretase), Notch1, and Hes1 genes.

MATERIALS AND METHODS

Animal Treatments

All animal-related activities for this study were reviewed and approved by the Institutional Animal Care and Use Committee (ACUC) and were designed to prevent or minimize any unnecessary animal discomfort. Female Charles River Sprague–Dawley rats (approximately 10–11 weeks of age) were used for both studies. For the assessment of microanatomic gene expression in normal (untreated) rats, kidneys from four rats were collected. For the PA study, five female rats/group were administered a single intravenous (IV) dose of PA (Sigma Aldrich, St. Louis, MO) dissolved in 0.9% sodium chloride (NaCl) at 150 mg/kg body weight through the tail vein, and five additional rats received an equivalent volume of the vehicle (0.9% NaCl) intravenously and served as controls. A dose of 150 mg/kg PA IV was selected, as it is reported to produce marked proteinuria (peaking on days 9–10 postdose) in Sprague–Dawley or Wistar–Furth rats (22).

Body Weight

Animals were weighed prior to treatment with PA or 0.9% NaCl and on days 1, 3, 6, and 9 following treatment.

Clinical Pathology

To confirm PA-related proteinuria, urinalysis was performed on urine collected overnight (chilled) from all animals on day 10. Urine volume was determined, and urine total protein, creatinine, and microalbumin concentrations were assessed using an ADVIA 1800 (Siemens Healthcare Diagnostics, Inc.). Based on these measurements, urine total microalbumin output, microalbumin/creatinine ratios, and total protein output were calculated. Mean values for each parameter were calculated, and the means for PA-treated animals were compared to the controls using a two-tailed unpaired Student's *t* test.

Histology

All animals were euthanatized with isoflurane anesthesia followed by exsanguination. Kidneys were collected and immersion fixed in 10% neutral buffered formalin for 48 h. Kidneys were processed, embedded in paraffin, sectioned at 4 μm, stained with hematoxylin and eosin (H&E), and examined by light microscopy. Additional sections of kidney from all animals were stained with periodic acid Schiff (PAS) and hematoxylin and examined for changes in the glomerular basement membranes. Transmitted light images were captured using an Infinity 1-3MgPx camera and an Olympus AX80 microscope. To visualize protein droplets, representative glomeruli from H&E-stained slides were photographed using a Nikon C1+ laser scanning microscope using a 488-nm laser.

Laser Capture Microdissection

Kidneys were embedded in optimal cutting temperature (OCT) embedding compound and frozen in liquid nitrogen. Frozen tissues were sectioned at 8 μm and stained with the HistoGene LCM Frozen Section Staining Kit (MDS Analytical Technologies, Sunnyvale, CA). Areas of interest were microdissected in duplicate from serial sections using an Arcturus XT Laser Microdissection Instrument onto the thermoplastic film of CapSure HS LCM Caps (MDS Analytical Technologies). The following anatomic regions of kidney were microdissected: glomeruli, cortical tubules, and collecting ducts (Fig. 1). Caps containing microdissected tissue were snapped onto 0.5-ml microcentrifuge tubes and stored frozen at −80°C. Serial sections of OCT-embedded whole kidneys were collected in separate 0.5-ml microcentrifuge tubes and processed alongside the microdissected samples to calibrate gene expression to that of the whole organ.

RT-PCR

To isolate RNA, samples were incubated with 20 (microdissected tissues) or 60 μl (whole organ sections) of TRIzol (Invitrogen, Carlsbad, CA) per sample for 30 min at 42°C. The homogenate was mixed with 10% chloroform and centrifuged at 12,000 × *g* for 10 min at 4°C to collect the organic phase. Organic-phase aliquots were

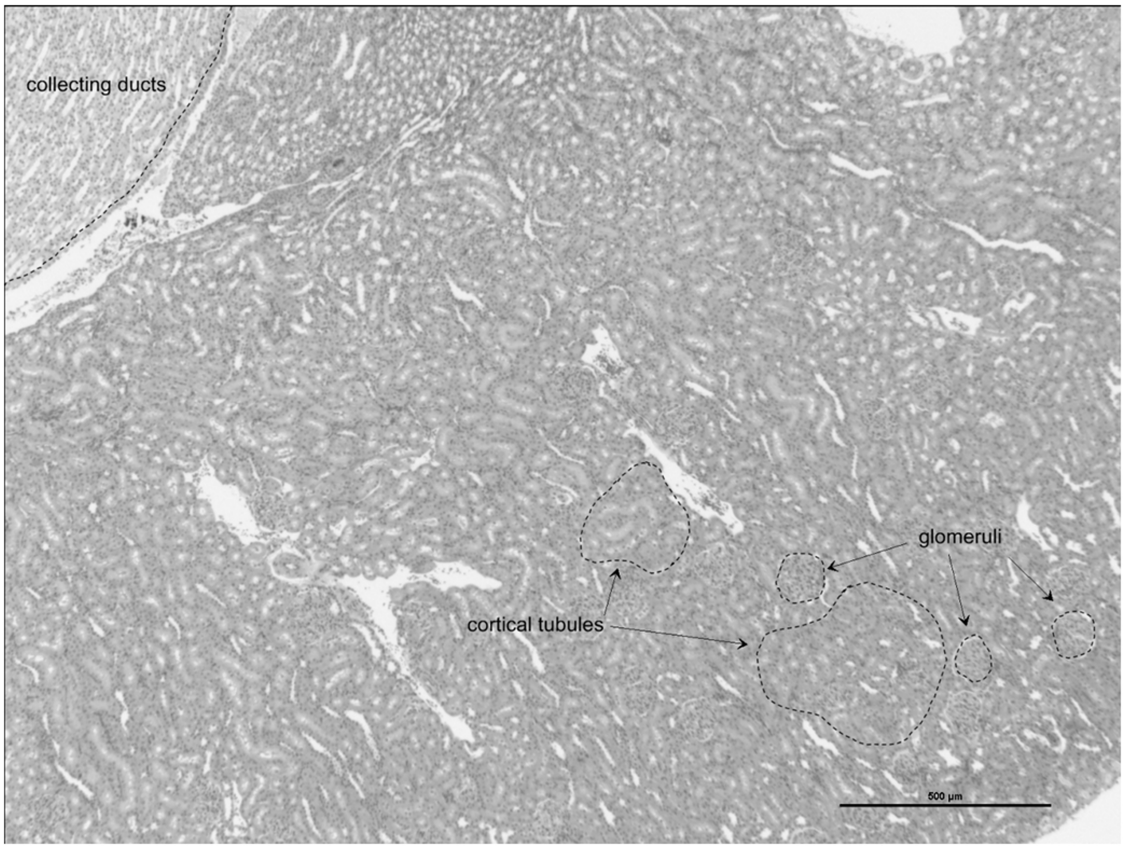

Figure 1. Kidney LCM. Representative regions (dotted lines) in the kidney sampled using laser capture microdissection (LCM). Target gene expression from microdissected regions was compared to that of serial sections of whole kidney. H&E stain; original magnification: 20×.

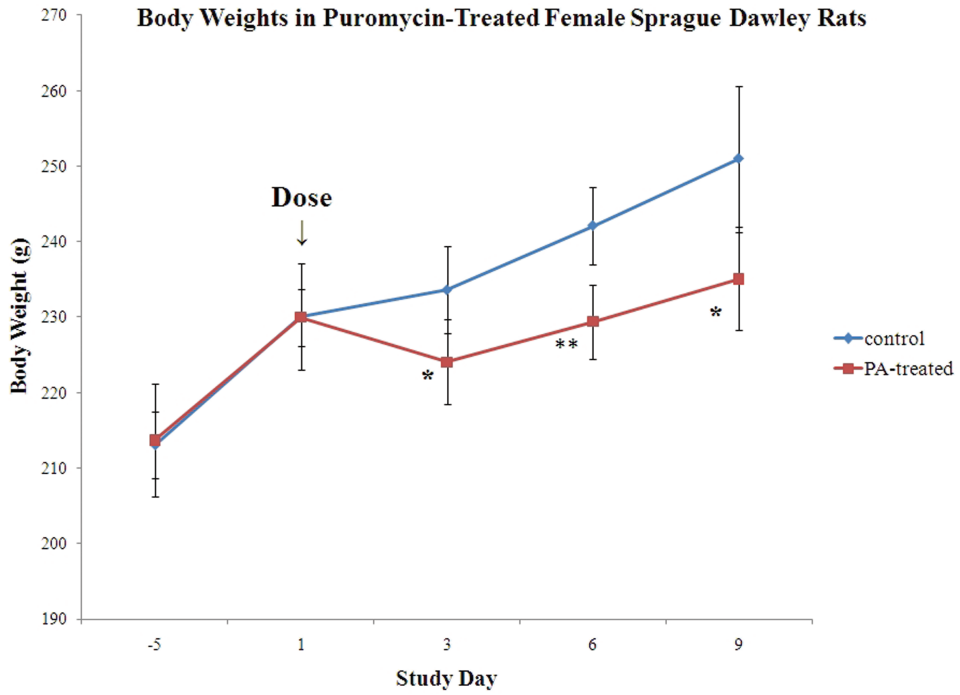

Figure 2. Body weights in control (0.9% sodium chloride) and puromycin (PA)-treated (150 mg/kg) female Sprague–Dawley rats. Puromycin treatment decreased mean body weights by day 3 after treatment; however, body weight gains returned to near control levels by day 6, but mean body weights remained significantly lower than vehicle controls through day 9. *$p<0.05$, ** $p<0.01$ (statistical difference from controls).

transferred to a MagMAX Express-96 Magnetic Particle Processor (Applied Biosystems, Carlsbad, CA) for automated RNA isolation. RNA was quantified (in ng/µl) using a Nanodrop spectrophotometer (Thermo Scientific, Wilmington, DE), and RNA purity was assessed from the resulting 260/280 nm ratio. Reverse transcription was performed using an iCycler iQ real-time PCR detection system (Bio-Rad, Hercules, CA) and the qScript cDNA Mix (Quanta, Gaithersburg, MD). The final concentration of RNA for each reaction mix was 12.5 ng/µl, and the cycling conditions were as follows: 5 min at 25°C, 30 min at 42°C, and 5 min at 85°C. Polymerase chain reaction was performed using the PerfeCta qPCR MasterMix UNG, ROX (Quanta) on an ABI 7900 (Applied Biosystems) using a "fast plate" setting. The following thermal cycler program was used: 2 min at 45°C, 30 s at 95°C, and 40

Table 1. Urinary Measurements in Control and PA-Treated Female Rats

Parameter Measured	Treatment	Day 10
Urine volume (ml)	Vehicle	10 ± 5
	Puromycin	7 ± 4
Urinary creatine (mg/dl)	Vehicle	51.48 ± 17.19
	Puromycin	79 ± 26.14
Total protein (mg/dl)	Vehicle	15 ± 5
	Puromycin	2060 ± 1209*
Total protein output (mg/collection time)	Vehicle	1.3 ± 0.2
	Puromycin	130.3 ± 89.5*
Urinary µ-albumin (mg/dl)	Vehicle	1.14 ± 0.6
	Puromycin	21.01 ± 5.61*
URMA/UCRE ratio	Vehicle	0.02 ± 0.01
	Puromycin	0.31 ± 0.16*
Total urinary µ-albumin (mg/collection time)	Vehicle	0.1 ± 0.05
	Puromycin	1.4 ± 0.81*

Statistical significance determined by the Student's *t* test. URMA = Urinary µ-albumin. UCRE = Urinary Creatine. Collection time = 18 h.
*Puromycin versus vehicle groups, $p<0.01$.

cycles of 2 s at 95°C and 20 s at 60°C. All TaqMan primer/probe sets were purchased from Applied Biosystems.

RESULTS

Body Weight

PA treatment (150 mg/kg) caused transient decreases (2.5–4%) in body weights by day 3 after dosing (Fig. 2). Body weight gains returned to near control levels by day 6 after treatment, although mean body weights remained significantly lower than controls through day 9 after dosing.

Urine Protein

Significantly increased ($p < 0.01$) urine microalbumin concentrations (18-fold compared to control), output (14-fold), and creatinine ratios (16-fold) were observed in PA-treated rats by 10 days after a single dose of 150 mg/kg (Table 1). Urine total protein (UTP) concentrations and output also increased significantly (137- and 100-fold, respectively) by 10 days after PA treatment. Urine volume and urinary creatinine levels were not significantly changed with PA treatment.

Histology

PA-related microscopic changes in glomeruli were limited to the presence of PAS-positive proteinaceous droplets likely within podocytes and mesangial cells (Fig. 3A and B). Proteinaceous casts were observed within tubules of the inner medulla and were likely related to protein leakage through injured glomeruli and impaired resorption through injured proximal tubular epithelium. Additional PA-related microscopic changes in the kidneys included tubular epithelial regeneration, vacuolation, and proteinaceous droplets

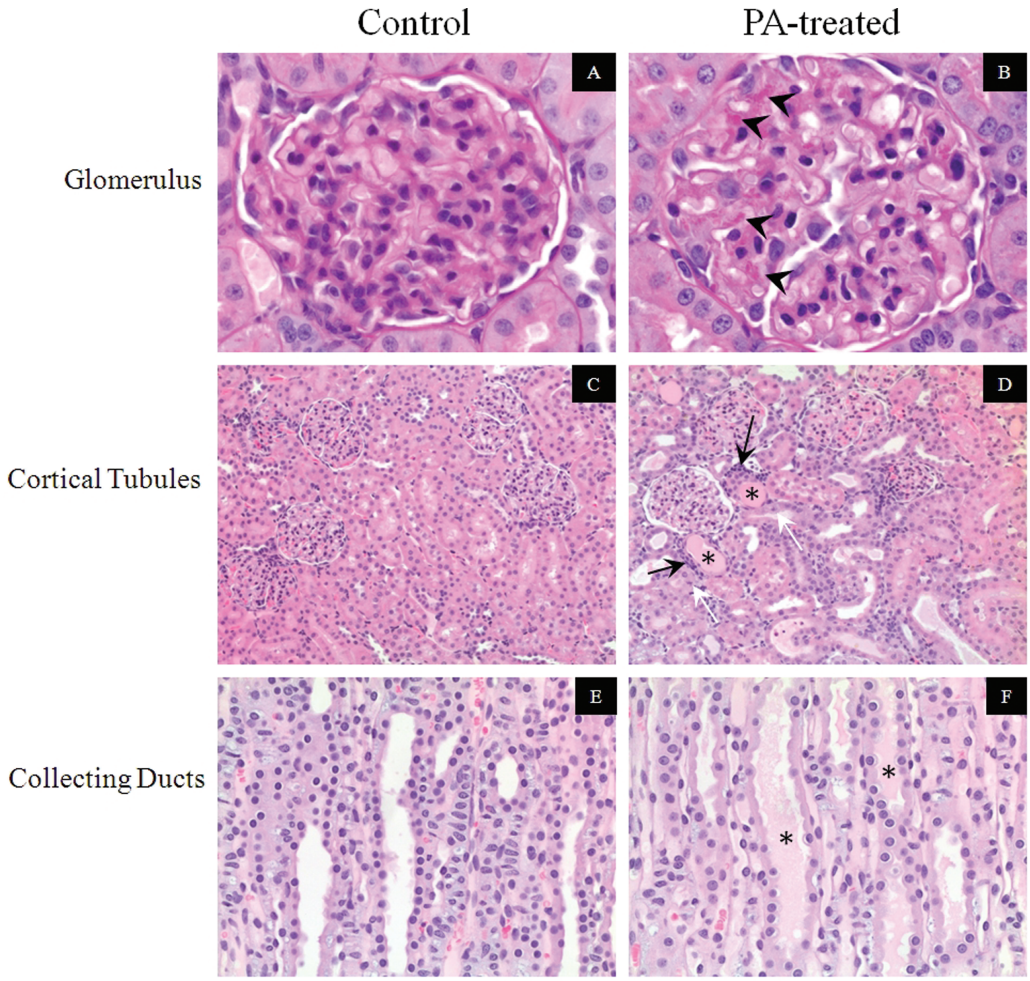

Figure 3. (A) Glomerulus from control rat is microscopically unremarkable. (B) Puromycin (PA) treated (150 mg/kg). Protein droplets (arrowheads) are present in glomeruli, likely within podocytes and mesangial cells. (C) Glomeruli, cortical tubules, and collecting ducts are morphologically normal. (D) PA-related proximal tubular changes include proteinaceous casts (*), epithelial regeneration with mitotic figures (white arrows), and interstitial mononuclear cell infiltrates (black arrows). (E) Collecting ducts are microscopically unremarkable. (F) PA 150 mg/kg. Collecting duct epithelium is microscopically unremarkable [compare with (E)], but tubular lumens contain occasional proteinaceous casts (*). (A, B) Periodic acid Schiff-hematoxylin stain, original magnification: 400×. (C, D) Hematolylin and eosin (H&E) stain, original magnification: 100×. (E, F) H&E stain, original magnification: 200×.

within the tubular epithelial cells and mononuclear cell infiltration in the interstitium (Fig. 3C–F). These microscopic changes were consistent with those previously reported for PA administration in rats (30–32). The kidneys from control rats were unremarkable microscopically.

Microanatomic Gene Expression

As a positive control for enrichment of glomeruli by LCM and for methods validation, the mRNA expression of podocin, a 383-amino acid integral membrane protein component of the glomerular slit diaphragm (33), was assessed (Fig. 4A). In a preliminary experiment, microdissected samples of glomeruli had substantially higher expression (>550-fold vs. whole kidney lysate) of podocin compared to microdissected samples of cortical tubules or collecting ducts from the same kidney.

In untreated adult rat kidneys, relative Notch1 expression was highest in the glomeruli followed by collecting ducts with lowest expression in cortical tubules (Fig. 4B). Hes1 and Presenilin1 (γ-secretase) expression were highest in the collecting ducts followed by cortical tubules and glomeruli (Fig. 4C and D). Presenilin1 expression in the collecting ducts was approximately fivefold higher compared to glomeruli and cortical tubules. Hes1 expression was approximately 7- and 10-fold higher in the collecting ducts versus cortical tubules or glomeruli, respectively.

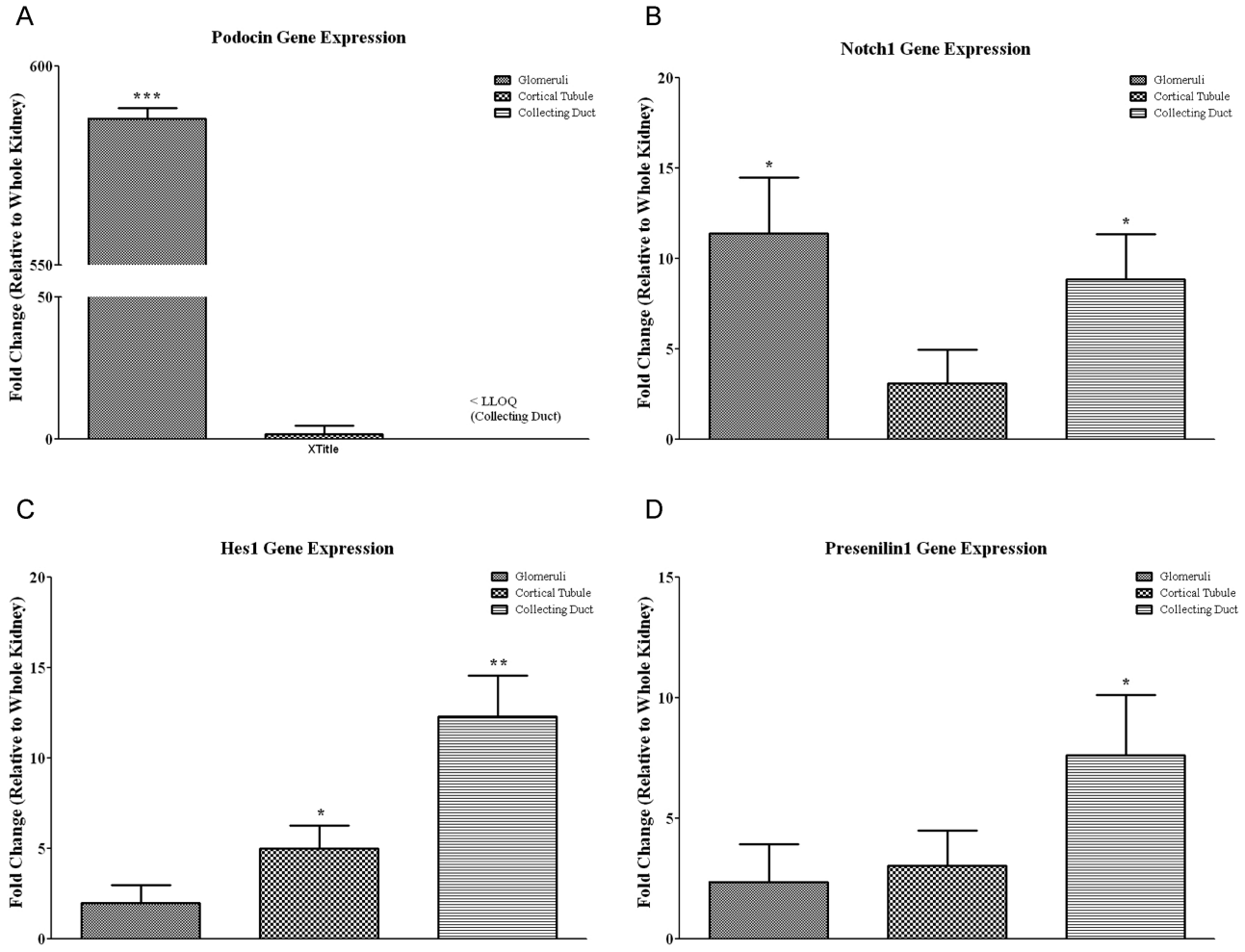

Figure 4. (A) Expression of Podocin1 mRNA (relative to whole kidney) in kidney from untreated adult female Sprague–Dawley rats ($n=4$). LLOQ: less than the lower limit of quantification. ***$p<0.001$ compared to the whole kidney lysate; unpaired Student's t test. (B) Expression of Notch1 mRNA (relative to whole kidney) in glomeruli, cortical tubules, and collecting ducts from untreated adult female Sprague–Dawley rats ($n=4$). *$p<0.05$ compared to the whole kidney lysate; unpaired Student's t test. (C) Expression of Hes1 mRNA (relative to whole kidney) in glomeruli, cortical tubules, and collecting ducts from untreated adult female Sprague–Dawley rats ($n=4$). *$p<0.05$, **$p<0.01$ compared to the whole kidney lysate; unpaired Student's t test. (D) Expression of Presenilin1 mRNA (relative to whole kidney) in glomeruli, cortical tubules, and collecting ducts from untreated adult female Sprague–Dawley rats ($n=4$). *$p<0.05$ compared to the whole kidney lysate; unpaired Student's t test.

Kidneys from rats treated with vehicle or 150 mg/kg of PA were microdissected and evaluated for the expression of Presenilin1, Notch1, and Hes1 (Fig. 5). Ten days post-PA treatment, the expression of Hes1 statistically increased ($p<0.05$) in the glomeruli (3.5-fold) and the tubules (2.2-fold) compared to the collecting ducts where no microscopic injury was observed. When compared to vehicle controls, Hes1 gene expression increased slightly (2.1-fold, $p=0.1$) in the glomeruli with minimal to no changes in the cortical tubules or collecting ducts. No significant Notch1 gene expression changes were detected in any of the microdissected regions. Presenilin1 expression was slightly increased 2- and 1.5-fold (not statistically significant) in the cortical tubules and glomerulus, respectively.

DISCUSSION

The present study focused on the gene expression pattern of the Notch signaling pathway from microdissected regions of the adult rat kidney. Gene expression of Presenilin1 (the catalytic component of γ-secretase complex), Notch1 (representative of Notch family of receptors), and Hes1 (a downstream target of activated Notch) was evaluated in the kidneys of untreated and PA-treated adult female rats. Using LCM, three microdissected regions of the kidney (glomerulus, cortical tubules, and collecting ducts) were isolated and processed for gene expression by RT-PCR. In untreated rats, the expression of Hes1 was lowest in the glomeruli, slightly greater in the cortical tubules, and highest in the collecting ducts. Others have reported similar findings showing detectible Notch activity and cleavage (34) in untreated mouse kidneys, with significant activation of Notch in the glomeruli of adult mice (7,8) following a low-level injury. The present study also demonstrated significant Hes1 expression (and therefore significant Notch activity) in the collecting duct in normal adult rats. Although Notch has been shown to play a critical role in collecting duct development (35), the role of Notch activation in collecting duct function in adult rats has not been elucidated. It is possible that Notch/Hes may play a role in keeping the renal progenitor cell population in an undifferentiated state. Indeed, recent reports showed the presence of a slow cycling population of cells in the collecting ducts (36,37), which have been proposed to act as resident progenitor cells that can terminally differentiate following injury/repair (38). Presenilin1 relative gene expression was used as an indicator of the overall γ-secretase complex levels. In untreated rats, Presenilin1 mRNA was detected in glomeruli, cortical tubules, and collecting ducts as well as the

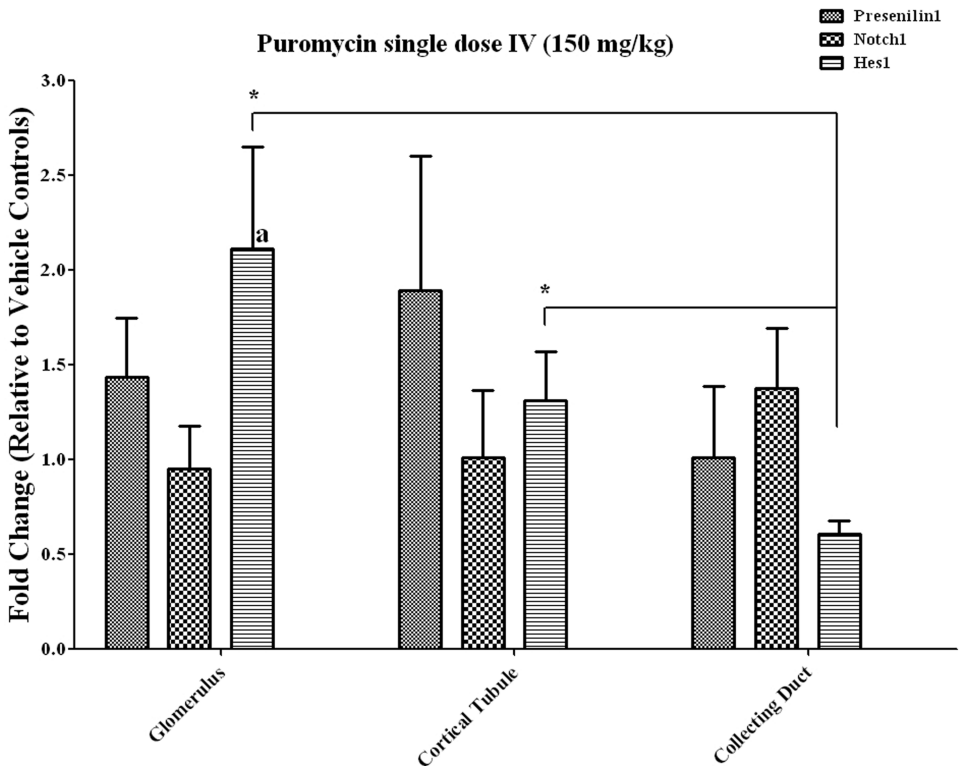

Figure 5. Expression of Presenilin1, Notch1, and Hes1 mRNA in glomeruli, cortical tubules, and collecting ducts following a single dose of puromycin. Adult female Sprague–Dawley rats ($n=4$). $^{a}p=0.1$, compared to vehicle treated controls; $^{*}p<0.05$ Hes1 expression in glomerulus compared to collecting duct; unpaired Student's *t* test.

whole kidney lysate; the highest expression relative to the whole kidney was in the collecting ducts. The gene expression pattern of Notch1 was similar to Presenilin1 except in the glomeruli where relative expression of Notch1 was notably higher. This higher expression of Notch1 in the glomeruli (relative to the whole kidney lysates) may reflect the potentially greater exposure of this region of the kidney to stimuli such as increased blood pressure, oxidative stress, and xenobiotics (39–43).

In order to evaluate microanatomic expression of the Notch pathway following injury, gene expression in rats was evaluated 10 days after a single intravenous dose of PA that produced significant proteinuria and histological changes of renal injury. PA-induced glomerular injury led to a slight increase of Notch activation in the glomerulus as indicated by an increase in Hes1 gene expression (2.1-fold; $p = 0.1$). Although not significantly increased compared to vehicle control, this relatively small increase in Hes1 expression does correlate with the histological observations of only minimal PA-induced glomerular injury. In addition, this change in Hes1 expression in the glomerulus (target microanatomic region) was greater than the collecting duct (no PA-induced effects) >3.5-fold ($p < 0.01$) (Fig. 5). The minimal trend for increased Hes1 expression (without statistical significance) seems to support reports by Niranjan et al. and Ueno et al. showing that Notch signaling is significantly increased only in glomerular apoptosis, possibly during infiltration of precursor cells in response to more severe damage (7,11). Comparatively, human MCD leads to a significant proteinuria mainly caused by glomerular functional effects (loss of podocyte foot processes leading to impairment of size/charge exclusion) and not by podocytes loss; therefore, the activation of Notch pathway necessary for podocyte replacement and differentiation would be limited. Indeed, the magnitude of Hes1 gene expression and histological findings were both relatively low. Others have shown that the expression and activation of Notch in injured kidneys is treatment and dose dependent, with FSGS-like glomerular injury in mice leading to significant Notch1 and Hes1 upregulation mostly due to necessary regenerative mechanisms whereby inhibition of Notch prevented mesenchymal phenotypic changes and cell migration to compensate for the injured filtration barrier in vivo (11). Further evidence of a role for Notch in repair of renal injury is highlighted in the present study with the significantly greater increase in Hes1 expression in the cortical tubules (PA-induced histological effects observed) compared to the collecting ducts (no histological lesion observed). Finally, although 10 days post-PA treatment has been reported as optimal for developing proteinuria and therefore clinical/functional effects (23), it may not reflect the greatest PA-induced gene expression changes, which could have peaked at an earlier time point.

This work shows that, in normal adult rat kidneys, collecting ducts contain the highest level of Presenilin1 (γ-secretase) and Hes1 expression while Notch1 expression is highest in glomeruli. Renal injury induced by a single dose of PA (150 mg/kg) included significant proteinuria and limited morphological changes, mostly in glomeruli and cortical tubules. Compared to the microscopically uninjured collecting ducts in these rats, Hes1 gene expression was increased in glomeruli and cortical tubules. Finally, this work demonstrates that evaluation of the gene expression pattern in specific regions of heterogeneous tissues such as kidneys may help in further understanding the role individual tissue regions play in the whole tissue homeostasis.

ACKNOWLEDGMENTS: The authors thank David Slinker, Julie Stevens, and the technical staff in Histology, Toxicology, Clinical Pathology, and Central Pharmacy in Drug Safety Evaluation, Mt. Vernon, IN, USA.

REFERENCES

1. Kaether C, Haass C, Steiner H. Assembly, trafficking and function of gamma-secretase. Neurodegener Dis 2006; 3:275–283.
2. Hardy J, Allsop D. Amyloid deposition as the central event in the aetiology of Alzheimer's disease. Trends Pharmacol Sci 1991; 12:383–388.
3. Skovronsky DM, Lee VM, Trojanowski JQ. Neurodegenerative diseases: New concepts of pathogenesis and their therapeutic implications. Annu Rev Pathol 2006; 1:151–170.
4. Artavanis-Tsakonas S, Rand MD, Lake RJ. Notch signaling: Cell fate control and signal integration in development. Science. 1999; 284:770–776.
5. Bray SJ. Notch signalling: A simple pathway becomes complex. Nat Rev Mol Cell Biol 2006; 7:678–689.
6. Cheng HT, Kopan R. The role of Notch signaling in specification of podocyte and proximal tubules within the developing mouse kidney. Kidney Int 2005; 68:1951–1952.
7. Niranjan T, Bielesz B, Gruenwald A, Ponda MP, Kopp JB, Thomas DB, et al. The Notch pathway in podocytes plays a role in the development of glomerular disease. Nat Med 2008; 14:290–298.
8. Vooijs M, Ong CT, Hadland B, Huppert S, Liu Z, Korving J, et al. Mapping the consequence of Notch1 proteolysis in vivo with NIP-CRE. Development 2007; 134:535–544.
9. Lasagni L, Ballerini L, Angelotti ML, Parente E, Sagrinati C, Mazzinghi B, et al. Notch activation differentially regulates renal progenitors proliferation and differentiation toward the podocyte lineage in glomerular disorders. Stem Cells 2010; 28:1674–1685.
10. Murea M, Park JK, Sharma S, Kato H, Gruenwald A, Niranjan T, et al. Expression of Notch pathway proteins correlates with albuminuria, glomerulosclerosis, and renal function. Kidney Int 2010; 78:514–522.
11. Ueno T, Kobayashi N, Nakayama M, Takashima Y, Ohse T, Pastan I, et al. Aberrant Notch1-dependent effects on glomerular parietal epithelial cells promotes collapsing focal

segmental glomerulosclerosis with progressive podocyte loss. Kidney Int 2013; 83:1065–1075.
12. Schmitz PG, O'Donnell MP, Kasiske BL, Katz SA, Keane WF. Renal injury in obese Zucker rats: Glomerular hemodynamic alterations and effects of enalapril. Am J Physiol 1992; 263:F496–F502.
13. Waters AM, Wu MY, Onay T, Scutaru J, Liu J, Lobe CG, et al. Ectopic notch activation in developing podocytes causes glomerulosclerosis. J Am Soc Nephrol 2008; 19:1139–1157.
14. Kato H, Susztak K. Repair problems in podocytes: Wnt, Notch, and glomerulosclerosis. Semin Nephrol 2012; 32:350–356.
15. Kim YH, Goyal M, Kurnit D, Wharram B, Wiggins J, Holzman L, et al. Podocyte depletion and glomerulosclerosis have a direct relationship in the PAN-treated rat. Kidney Int 2001; 60:957–968.
16. Ronconi E, Sagrinati C, Angelotti ML, Lazzeri E, Mazzinghi B, Ballerini L, et al. Regeneration of glomerular podocytes by human renal progenitors. J Am Soc Nephrol 2009; 20:322–332.
17. Sirin Y, Susztak K. Notch in the kidney: Development and disease. J Pathol 2012; 226:394–403.
18. Appel D, Kershaw DB, Smeets B, Yuan G, Fuss A, Frye B, et al. Recruitment of podocytes from glomerular parietal epithelial cells. J Am Soc Nephrol 2009; 20:333–343.
19. Humphreys BD, Czerniak S, DiRocco DP, Hasnain W, Cheema R, Bonventre JV. Repair of injured proximal tubule does not involve specialized progenitors. Proc Natl Acad Sci USA 2011; 108:9226–9231.
20. Lasagni L, Romagnani P. Glomerular epithelial stem cells: The good, the bad, and the ugly. J Am Soc Nephrol 2010; 21:1612–1619.
21. Caulfield JP, Reid JJ, Farquhar MG. Alterations of the glomerular epithelium in acute aminonucleoside nephrosis. Evidence for formation of occluding junctions and epithelial cell detachment. Lab Invest 1976; 34:43–59.
22. Pippin JW, Brinkkoetter PT, Cormack-Aboud FC, Durvasula RV, Hauser PV, Kowalewska J, et al. Inducible rodent models of acquired podocyte diseases. Am J Physiol Renal Physiol 2009; 296:F213–F229.
23. Olson JL, Rennke HG, Venkatachalam MA. Alterations in the charge and size selectivity barrier of the glomerular filter in aminonucleoside nephrosis in rats. Lab Invest 1981; 44:271–279.
24. Shiiki H, Sasaki Y, Nishino T, Kimura T, Kurioka H, Fujimoto S, et al. Cell proliferation and apoptosis of the glomerular epithelial cells in rats with puromycin aminonucleoside nephrosis. Pathobiology 1998; 66:221–229.
25. Grond J, Weening JJ, Elema JD. Glomerular sclerosis in nephrotic rats. Comparison of the long-term effects of adriamycin and aminonucleoside. Lab Invest 1984; 51:277–285.
26. Marshall CB, Pippin JW, Krofft RD, Shankland SJ. Puromycin aminonucleoside induces oxidant-dependent DNA damage in podocytes in vitro and in vivo. Kidney Int 2006; 70:1962–1973.
27. Shah SV. Role of reactive oxygen metabolites in experimental glomerular disease. Kidney Int 1989; 35:1093–1106.
28. Diamond JR, Bonventre JV, Karnovsky MJ. A role for oxygen free radicals in aminonucleoside nephrosis. Kidney Int 1986; 29:478–483.
29. Thakur V, Walker PD, Shah SV. Evidence suggesting a role for hydroxyl radical in puromycin aminonucleoside-induced proteinuria. Kidney Int 1988; 34:494–499.
30. Diamond JR, Karnovsky MJ. Focal and segmental glomerulosclerosis following a single intravenous dose of puromycin aminonucleoside. Am J Pathol 1986; 122:481–487.
31. Nagle RB, Bulger RE, Striker GE, Benditt EP. Renal tubular effects of the aminonucleoside of puromycin. Lab Invest 1972; 26:558–565.
32. Eddy AA, Michael AF. Acute tubulointerstitial nephritis associated with aminonucleoside nephrosis. Kidney Int 1988; 33:14–23.
33. Roselli S, Gribouval O, Boute N, Sich M, Benessy F, Attie T, et al. Podocin localizes in the kidney to the slit diaphragm area. Am J Pathol 2002; 160:131–139.
34. Sharma S, Sirin Y, Susztak K. The story of Notch and chronic kidney disease. Curr Opin Nephrol Hypertens 2011; 20:56–61.
35. Jeong HW, Jeon US, Koo BK, Kim WY, Im SK, Shin J, et al. Inactivation of Notch signaling in the renal collecting duct causes nephrogenic diabetes insipidus in mice. J Clin Invest 2009; 119:3290–3300.
36. Oliver JA, Maarouf O, Cheema FH, Liu C, Zhang QY, Kraus C, et al. SDF-1 activates papillary label-retaining cells during kidney repair from injury. Am J Physiol Renal Physiol 2012; 302:F1362–F1373.
37. Oliver JA, Klinakis A, Cheema FH, Friedlander J, Sampogna RV, Martens TP, et al. Proliferation and migration of label-retaining cells of the kidney papilla. J Am Soc Nephrol 2009; 20:2315–2327.
38. Fesenko I, Franklin D, Garnett P, Bass P, Campbell S, Hardyman M, et al. Stem cell marker TRA-1-60 is expressed in foetal and adult kidney and upregulated in tubulointerstitial disease. Histochem Cell Biol 2010; 134:355–369.
39. Kitada K, Nakano D, Liu Y, Fujisawa Y, Hitomi H, Shibayama Y, et al. Oxidative stress-induced glomerular mineralocorticoid receptor activation limits the benefit of salt reduction in Dahl salt-sensitive rats. PLoS One 2012; 7:e41896.
40. Khazim K, Gorin YC, de Cassia Cavaglieri R, Abboud HE, Fanti P. The antioxidant silybin prevents high glucose-induced oxidative stress and podocyte injury in vitro and in vivo. Am J Physiol Renal Physiol 2013; 305: F691–F700.
41. Matsusaka T, Sandgren E, Shintani A, Kon V, Pastan I, Fogo AB, et al. Podocyte injury damages other podocytes. J Am Soc Nephrol 2011; 22:1275–1285.
42. Robertson JL. Chemically induced glomerular injury: A review of basic mechanisms and specific xenobiotics. Toxicol Pathol 1998; 26:64–72.
43. Nagase M, Shibata S, Yoshida S, Nagase T, Gotoda T, Fujita T. Podocyte injury underlies the glomerulopathy of Dahl salt-hypertensive rats and is reversed by aldosterone blocker. Hypertension 2006; 47:1084–1093.